Proceedings of ISFOG 2025
5TH INTERNATIONAL SYMPOSIUM ON
FRONTIERS IN OFFSHORE GEOTECHNICS
Nantes, France | June 9-13 2025

ISBN 978-2-85782-758-0

Dynamic Soil-Structure Interaction evaluations of liquefaction-induced settlements of a Pipeline End Manifold

Y. K. Chaloulos*, S. Giannakos, T. Limnaiou, C. Tsifis, A. Giannakou, J. Chacko
GR8 GEO, Athens, Greece

A. Meijer
Intecsea, The Hague, The Netherlands

G. Vazquez Perez, C. Hoffmann
VanOord, Rotterdam, The Netherlands

ychaloulos@gr8-geo.com (corresponding author)

ABSTRACT: The seismic performance of an offshore Pipeline End Manifold (PLEM) structure founded on liquefiable soils was analysed by means of simplified triggering analyses, 1D effective stress dynamic analyses and 3D Soil-Structure-Interaction (SSI) dynamic analyses. The numerical analyses employ the Ta-Ger constitutive model, calibrated against project specific test data, as well as state-of-the-art techniques. Results showed that simplified analyses can overestimate both the liquefaction potential and the associated settlements. While site response analyses produce more rational estimates of liquefaction potential, they can overestimate deformations as they do not account for 3D interaction effects. 3D dynamic analyses provide more rational deformation estimates showing that the overall seismic performance of the various components of the structure (i.e., PLEM foundation and pipelines) is not jeopardized as estimated settlements and horizontal displacements remain low.

Keywords: liquefaction; SSI; numerical modelling; PLEM

1 INTRODUCTION

This paper presents critical aspects of the seismic design of a Pipeline-End-Manifold (PLEM) adjacent to a Single Point Mooring (SPM) near a refinery in Central America, including effective stress site response analyses, assessments of post-liquefaction volumetric settlements and numerical evaluations of liquefaction-induced settlements.

3D fully coupled dynamic analyses were performed to assess the performance of the PLEM and evaluate the absolute co-seismic and post-seismic PLEM and PLEM-Pipeline settlements. These analyses allow for a more accurate evaluation of foundation settlements in comparison to simplified Cone Penetration Test (CPT) triggering and dynamic coupled effective stress site response analyses as they account for soil-foundation interaction while all three components of motion are applied at the base of the model.

2 SITE CHARACTERIZATION

The following main soil layers were encountered in CPTs and boreholes performed in the project area:

- A very soft clay layer extending from mudline to 1.5m depth (s_u=2-7kPa, V_s=30-60m/s).
- A firm to stiff clay layer encountered between 1.5 to 5m depth (s_u=40-50kPa, V_s=130-160m/s).
- A medium dense sand layer (D_r≈60%) with thin clay interlayers between 5-13m (V_s=160-220m/s).
- A very stiff clay layer between 13 to 16m depth (s_u=130-150kPa, V_s≈240m/s).
- Sequences of medium dense (D_r≈60%) to dense sands (D_r≈70-80%) from 16m to the maximum depth explored (~50m below mudline) with V_s=260-290m/s.

The Plasticity Index of the clay units and the unit weight ranged between PI=10-50% and γ=18-19kN/m^3 respectively. The permeability for the non-cohesive layers was k=5x10^{-5} m/s (Robertson 2009).

3 SIMPLIFIED LIQUEFACTION TRIGGERING ASSESSMENTS

Simplified liquefaction triggering analyses were performed to evaluate the liquefaction potential and to obtain preliminary estimates of liquefaction-induced volumetric settlements. The cyclic stress ratio employed in these analyses was directly estimated through total-stress nonlinear site response analyses where all layers were modeled with the General Quadratic/Hyperbolic (GQ/H) model (Groholski et al.

2016). Because the CPT tip resistances in the sand layers are impacted (lowered) by the thin clay interlayers, the inverse filtering process developed by Boulanger and DeJong (2018) was used to corect tip resistance and sleeve friction within the sand layers. It was found that the correction for the presence of thin cohesive layers on the measured tip resistance resulted in decreasing the liquefiable sand thickness by 5-30%.

Results from the simplified analyses are presented on Figure 1 showing potential for liquefaction primarily within the top 13m of granular soils with estimated factors of safety less than 1. It should be noted also that liquefaction might occur within the deeper medium dense sands but the potentially liquefiable layers are more limited in thickness.

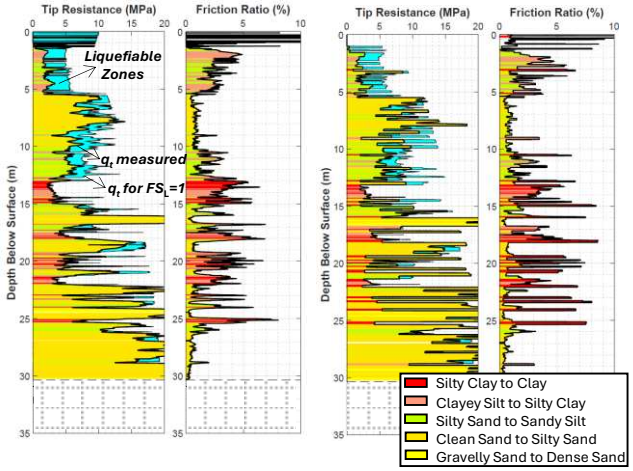

Figure 1. Liquefaction Triggering Assessment with Youd et al (2001) thin layer correction (left) and with Boulanger and DeJong (2018) inverse filtering (right)

4 EFFECTIVE STRESS SITE RESPONSE ANALYSES

4.1 Approach overview

Effective stress site response analyses were performed with the finite difference code FLAC (Itasca 2019a) to evaluate the effects of excess pore pressure development on ground motion estimates and obtain a more realistic assessment of the thickness of liquefiable soil layers and magnitude of post-liquefaction volumetric settlements.

The evaluation of post-seismic reconsolidation settlements was performed with the procedure outlined in Chaloulos et al. (2020). The methodology has been verified against the Port Island case study (Ishihara et al. 1996) and is based on the assignment of a constrained modulus corresponding to consolidation strains estimated from the maximum shear strains that developed during the earthquake based on the Ishihara and Yoshimine (1992) chart. The model is then brought into equilibrium producing post-seismic consolidation-related deformations.

Analyses were performed for an Abnormal Level Event (ALE) design level (ISO 2017) with a return period of T_{ret}=1400years.

The base case analyses ignored the thin clay layers within the sand layers. However, to evaluate the effect of the thin clay interlayers within the medium dense sand layers between 5 and 15m depth, additional analyses were performed incorporating a 0.2m-thick clay layer in every meter of sand (Figure 5).

4.2 Soil constitutive models and model calibration

The response of sand units was simulated with the Ta-Ger constitutive model (Tasiopoulou and Gerolymos 2016a; b). Ta-Ger can be regarded as a bounding single-surface model, within a smooth hysteresis framework avoiding classical elasto-plasticity requirements for an initial elastic response, an explicitly defined plastic modulus and a loading index. The formulation provides a definite and continuous expression of an elasto-plastic matrix, connecting the strain with the stress increment; thus, neither inversion of the strain-stress increment equation nor stress point algorithms and iterative procedures are required in numerical implementation, thus increasing computational efficiency. The model is implemented by GR8 GEO in FLAC and FLAC3D.

Ta-Ger was calibrated to capture liquefaction triggering and strain accumulation behavior observed in project-specific Cyclic Simple Shear (CSS) tests. Figure 2a compares numerical and experimental data in terms of liquefaction triggering while Figure 2b shows numerical estimates of post-liquefaction strains compared both against experimental data as well as the semi-empirical curves developed by Tasiopoulou et al. (2020).

At the same time, the calibrated model can reproduce the shear stress-strain response observed in the CSS tests (Figure 3). As shown on Figure 3d, at about 22 cycles where the value of shear strain exceeds 3%, the excess pore pressure value r_u has grown to 0.8-1 corresponding to effective stresses of approximately 0-20kPa. While the shear strains keep increasing, the effective stresses remain within this range, which is indicative of a liquefied state (cyclic mobility).

The conssistency between observed and simulated behavior suggests that the calibrated model can be tailored to adequately simulate cyclic soil behavior at element level in terms of liquefaction triggering and post-liquefaction shear strain accumulation but also in terms of stress-strain behavior observed in the tests.

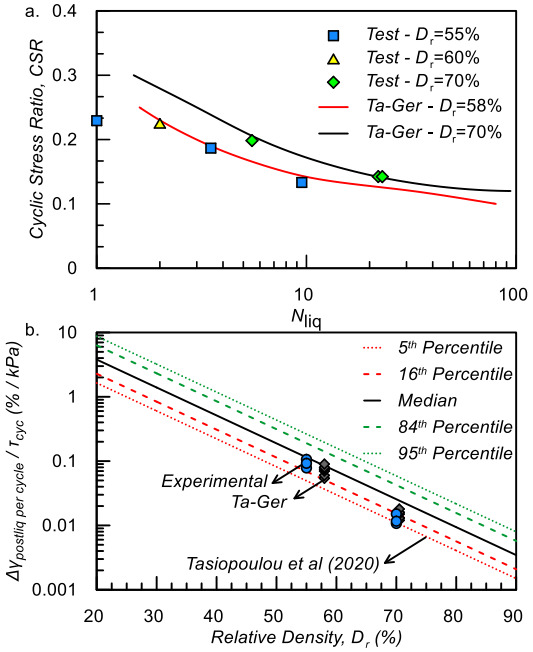

Figure 2. Liquefaction Resistance Curves and Post-liquefaction Shear Strain accumulation obtained from Ta-Ger single element simulations vs results from CSS Tests and Semi-empirical curves by Tasiopoulou et al (2020).

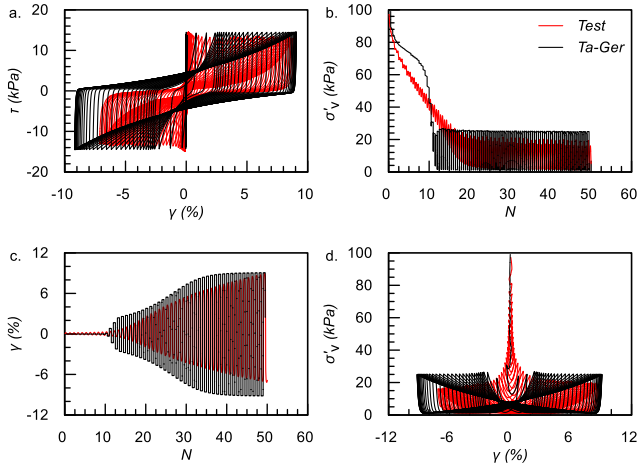

Figure 3. Comparison of Single Element Simulation with Ta-Ger and CSS Test Results: (a) τ vs γ, (c)γ vs N (b) σ'$_v$ vs N and (d) σ'$_v$ vs γ (D_r=58%)

Note that, apart from the comparisons shown herein, the Ta-Ger model can be calibrated to predict the post-liquefaction shear strain accumulation in sands for all ranges of relative densities and for fine-grained soils exhibiting sand-like behavior (i.e. low plasticity silts). It can also be calibrated to capture post-liquefaction strain accumulations that fall outside of the range of the dataset published by Tasiopoulou et al. (2020) (e.g., Chaloulos et al. 2023, 2024; Tasiopoulou et al. 2019, 2020, 2021, 2023).

The response of fine-grained materials is simulated with the GQ/H model also implemented by GR8 GEO in FLAC and FLAC3D. GQ/H adopts a hysteretic, nonlinear stress-strain law allowing for modelling reduction of the shear modulus and increase in hysteretic damping with increasing shear strain. Model parameters were calibrated against advanced dynamic tests performed on fine-grained samples comprising Resonant Column (RC) and Consolidated Undrained Strain-controlled CSS tests at 0.3% and 1.5% strain as shown on Figure 4.

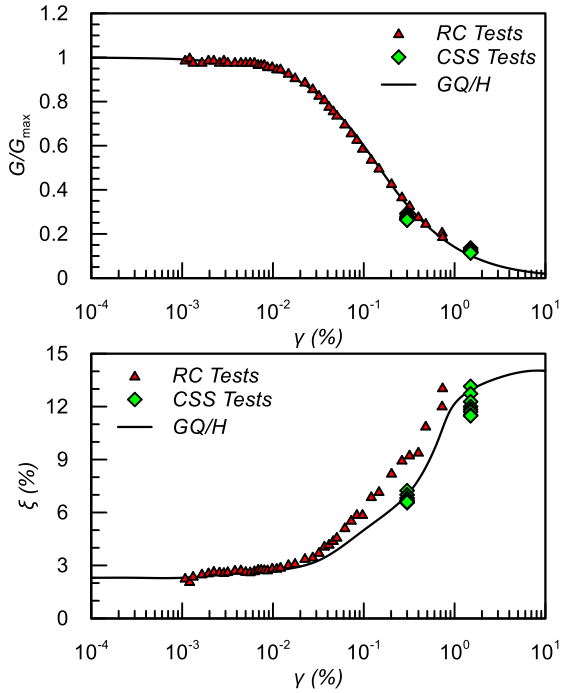

Figure 4. Calibrated GQ/H model against G/G_{max} and Damping Curves for Shallow Fine-grained Layers

4.3 Main Findings

Figure 5a presents the numerical model for the 1D effective stress site response analyses. Two types of analyses were performed i.e., without and with the presence of clay laminations within the medium dense sands between 5-13m depth (shown with brown).

As shown on Figure 5b, shear strains in excess of 3% (assumed threshold for liquefaction occurence) develop in parts of the medium dense sand layers (i.e., D_r=60%) when the presence of clay laminations is ignored (red lines). On the other hand, the maximum shear strains that develop in the profile including clay laminations (gray lines) are considerabley higher. This is primarily due to the creation of a water film at the interface between the sand and the clay (due to the development of excess pore water pressures within the liquefied sand) which results in the creation of a looser sand zone close to the interface as shown on the relative density contours at the end of shaking (Figure 5c). This phenomenon is also referred to as void redistribution. It is noted that the potential for void redistribution to cause significant shear deformations

decreases with increasing D_r, as a higher D_r has the combined benefits of reducing the volume of water expelled by contracting zones and increasing the volume of water that can be absorbed by dilating zones. For situations in which void redistribution is significant, it is expected that the shear strength will drop to a small fraction of the pre-earthquake shear strength, because the impeded pore water seepage allows the soil to shear at a sustained low value of vertical effective stress. The effects of clay laminations were further incorporated in the subsequent 3D analyses to assess the post-earthquake stability of the system as discussed in Section 5.1.

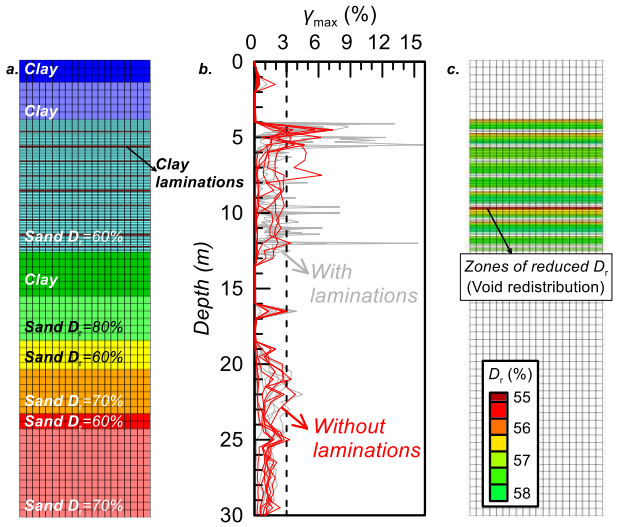

Figure 5. Influence of Clay Laminations on Maximum Shear Strains

5 3D EVALUATIONS OF PLEM FOUNDATION PERFORMANCE

5.1 Numerical Approach

Figure 6 shows the numerical model built for the 3D effective-stress, dynamic analyses performed with FLAC3D (Itasca 2019b) to assess the magnitude of seismic and post-seismic settlements of the PLEM foundation as well as the corresponding differential settlements between the PLEM foundation and the pipelines. The intent of the analyses was to evaluate the performance of the structure/foundation system accounting both for soil-foundation interaction and the concurrent action of all three seismic components.

The seismic performance of the PLEM was evaluated both during and after the earthquake. The first stage (co-seismic) involved performing dynamic, nonlinear, effective stress analyses to estimate the liquefied zones and the deformations that occur during shaking. Sand and sand-like deposits were modelled using Ta-Ger and clay deposits using GQ/H. The second stage involved both the estimation of post-seismic liquefaction-induced volumetric settlements (see Section 4.1) as well as the evaluation of the overall stability of the system. For the latter, a static analysis was performed in which the liquefied zones were assigned a residual strength (Idriss and Boulanger, 2008). Note that the adopted residual value accounts for void redistribution effects which are prominent in the present case.

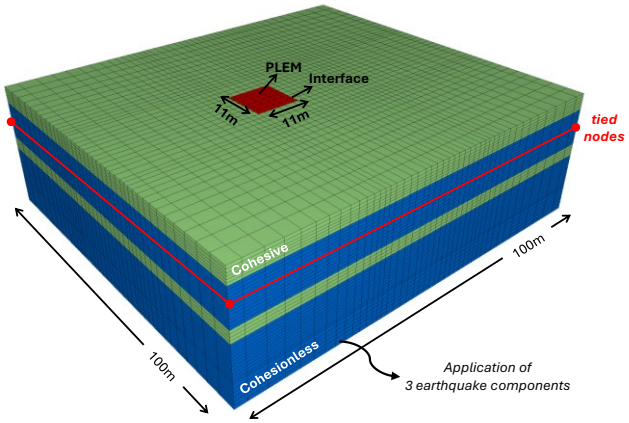

Figure 6: 3D numerical model showing the different soil units and the PLEM

The PLEM was simulated as an 11x11m uniform square slab using isotropic elastic shell elements (E=210GPa, ν=0.3) connected to the grid through an interface element. For its inertial response a total mass of M_{tot}=102 mT corresponding to its total weight was considered. An interface friction angle of 29° and zero tensile strength was assigned to the interfaces. Note that the pipeline was not included in the analysis as its interaction with the soil is not expected to significantly affect the estimated defoemations. Finally, all three components of ground motion were applied at the base of the model while tied-node boundary conditions were used at the vertical boundaries of the model.

5.2 Co-Seismic response

Figure 7a and 7b show contours of maximum shear strain and excess pore pressure ratio r_u at the end of shaking along a vertical cross-section through the PLEM. Similar to the 1D effective-stress site response analyses (also shown on the figure), considerable shear strains (>3%) related to soil liquefaction develop in the upper sand layer located at 5-13m depth with relative density D_r=60%.

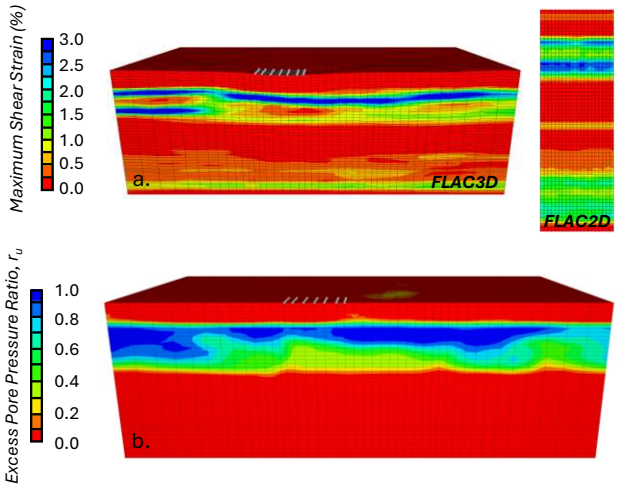

Figure 7: (a) Deformed Mesh and Contours of Maximum Shear Strain from the 3D and 1D Numerical Analyses (b) Contours of excess pore pressure ratio r_u

Figure 8 shows contours of vertical displacements at the end of shaking (co-seismic) showing the development of considerable deformations only within the clay layers indicating that negligible shear-induced settlements develop within the liquefiable sand. This can be attributed to the relatively low foundation pressure (i.e. 5kPa) and the presence of non-liquefiable soils (i.e. a crust) directly under the foundation.

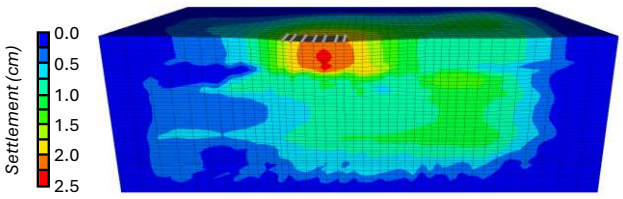

Figure 8: Contours of Vertical Displacement at the end of shaking

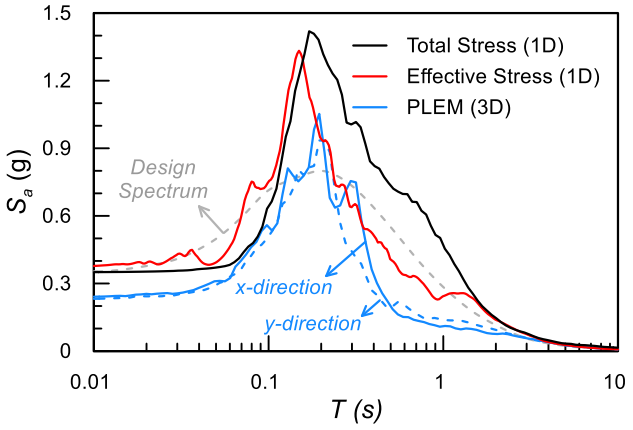

Figure 9: Response Spectra at the Ground Surface from the 1D and the 3D Analyses.

Figure 9 compares acceleration response spectra at the PLEM location from the 3D and the 1D analyses. The presence of the PLEM is beneficial as it reduces spectral accelerations across the entire range of periods due to soil-structure interaction.

5.3 Post-Seismic response

Figure 10 presents the time history of the accumulation of PLEM settlements during and after the earthquake (co-seismic and volumetric). Figure 11 compares post-seismic volumetric settlements estimated from simplified liquefaction triggering assessment, 1D site response analyses and 3D SSI analyses. Simplified procedures substantially overestimate volumetric settlements (note the logarithmic scale). 1D effective-stress analyses produce lower estimates as liquefaction of deeper layers results in motion de-amplification and thus decrease of the thickness of potentially liquefiable layers that actually liquefy. Finally, 3D SSI analyses further reduce the estimated settlements as they also account for the 3D nature of the problem and the soil and the soil-foundation interaction. Note that simplified analyses over-estimate volumetric settlements compared to 3D analyses by a factor of 10-25.

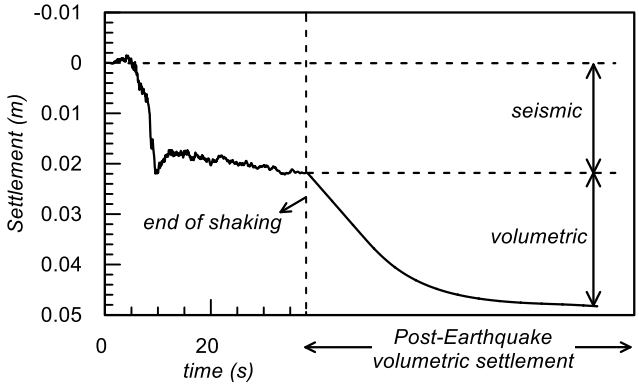

Figure 10. Time history of PLEM settlement during and after the end of the earthquake (co-seismic and volumetric)

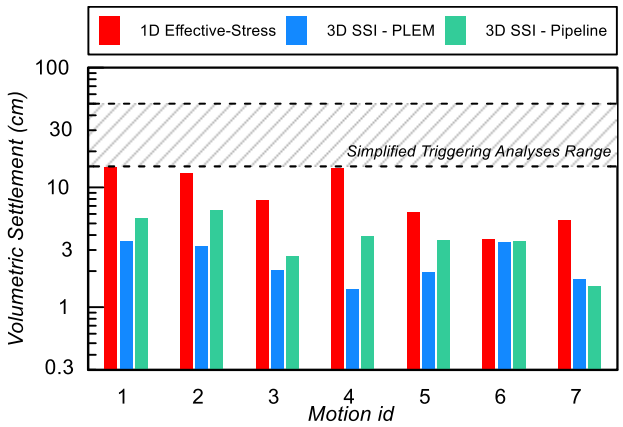

Figure 11. Comparison of Post-Liquefaction Volumetric Settlement from Simplified Liquefaction Triggering Analyses, 1D Effective Stress Analyses and 3D SSI analyses

As for post-earthquake stability, analyses showed that the system could reach a new equilibrium with the updated residual strength by developing only minor deformations i.e., without jeopardizing its stability.

5.4 PLEM and Pipeline Performance

The overall performance of the PLEM-pipeline system is summarized on Figure 12 and 13 in terms of total settlement and maximum horizontal displacement respectively at the PLEM, the PLEM-Pipeline connection as well as the PLEM-Pipeline differential displacement. The estimated PLEM and Pipeline settlements range between 2-6cm and 2-7cm, respectively, while the differential settlements are only 1cm or less. Horizontal displacements range between 1-6cm for both the PLEM and the PLEM-Pipeline connection, while the corresponding differential displacement is practically negligible.

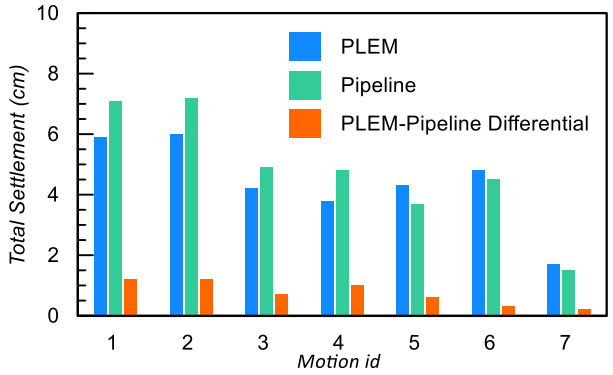

Figure 12: Total settlements (co-seismic and post-seismic)

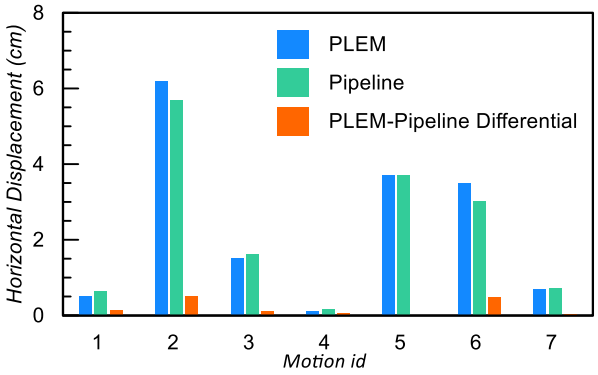

Figure 13: Maximum horizontal displacements

6 CONCLUSIONS

The seismic performance of an offshore subsea structure was analysed by means of simplified triggering analyses, 1D effective stress dynamic analyses and 3D SSI dynamic analyses. Results showed that simplified analyses can overestimate both the liquefaction potential and the associated settlements. Site response analyses on the other hand produce more rational estimates of liquefaction potential however they can overestimate deformations as they do not account for 3D interaction effects. 3D dynamic analyses provided a basis for directly assessing the impacts of ground motions on the PLEM/pipeline system, with the resulting absolute and relative deformations will within design tolerances.

AUTHOR CONTRIBUTION STATEMENT

Y.K. Chaloulos, S. Giannakos, C. I. Tsifis, T. I. Limnaiou, A. Giannakou, J. Chacko,: Software, Conceptualization, Methodology, Investigation, Writing-Original draft, **A. Meijer, G. Vazquez Perez, C. Hoffmann:** Writing-Reviewing and Editing

REFERENCES

Boulanger, R. W., and J. T. DeJong. 2018. “Inverse filtering procedure to correct cone penetration data for thin-layer and transition effects.” Cone Penetration Testing, 25–44. Delft University of Technology, The Netherlands.

Chaloulos, Y. K., A. Giannakou, V. Drosos, P. Tasiopoulou, J. Chacko, and S. de Wit. 2020. “Liquefaction-induced settlements of residential buildings subjected to induced earthquakes.” SDEE, 10.1016/j.soildyn.2019.105880

Chaloulos, Y. K., P. Tasiopoulou, T. Georgarakos, A. Giannakou, J. Chacko, and S. Unterseh. 2023. “3D Effective stress analyses of dynamic LNG tank performance on liquefiable soils improved with stone columns.” SDEE, 174. 10.1016/J.SOILDYN.2023.108170.

Chaloulos, Y. K., P. Tasiopoulou, A. Giannakou, J. Chacko, A. Aghakouchak, and S. T. 2024. “Fully-coupled Cyclic Time-History Analyses of Monopile Foundations in Sand.” Ocean Engineering, 298 (State of Practice – Geotechnical Considerations for Offshore Wind). 10.1016/j.oceaneng.2024.116691.

Groholski, D. R., Y. M. A. Hashash, B. Kim, M. Musgrove, J. Harmon, and J. P. Stewart. 2016. “Simplified Model for Small-Strain Nonlinearity and Strength in 1D Seismic Site Response Analysis.” J Geotec Geoenv Eng, 142 (9), 10.1061/(ASCE)GT.1943-5606.0001496.

Idriss, M. I., and R. W. Boulanger. 2008. *Soil Liquefaction During Earthquakes*. California, USA: EERI.

Ishihara, K., S. Yasuda, and H. Nagase. 1996. “Soil characteristics and ground damage.” Soils and Foundations, 10.3208/SANDF.36.SPECIAL_109.

Ishihara, K., and M. Yoshimine. 1992. "Evaluation of Settlements in Sand Deposits Following Liquefaction During Earthquakes." Soils and Foundations, 32 (1): 173–188. 10.3208/SANDF1972.32.173.

ISO 19901-2 (2017). Petroleum and natural gas industries - Specific requirements for offshore structures - Part 2: Seismic design procedures and criteria.

Itasca. 2019a. "FLAC - Fast Lagrangian Analysis of Continua, Ver. 8.1." Itasca Consulting Group Inc.

Itasca. 2019b. "FLAC3D - Fast Lagrangian Analysis of Continua in 3D, Ver. 7.0." Itasca Consulting Group Inc.

Robertson, P. K. 2009. "Interpretation of cone penetration tests — a unified approach." CGJ, 46 (11): 1337–1355. https://doi.org/10.1139/T09-065.

Tasiopoulou, P., and N. Gerolymos. 2016a. "Constitutive modeling of sand: Formulation of a new plasticity approach." SDEE, 10.1016/J.SOILDYN.2015.12.014.

Tasiopoulou, P., and N. Gerolymos. 2016b. "Constitutive modelling of sand: a progressive calibration procedure accounting for intrinsic and stress-induced anisotropy." Géotechnique, 66 (9) 10.1680/JGEOT.15.P.284.

Tasiopoulou, P., Y. K. Chaloulos, N. Gerolymos, A. Giannakou, and J. Chacko. 2019. "3D and 2D simulations of liquefaction-induced settlements of shallow foundations using Ta-Ger model." 7th International Conference on Earthquake Geotechnical Engineering. Rome, Italy.

Tasiopoulou, P., J. Chacko, Y. K. Chaloulos, and A. Giannakou. 2020. "Insight into the Cyclic Response of OWT Pile Foundations in Sand: Numerical Simulation of PISA Field Tests." 4th International Symposium on Frontiers in Offshore Geotechnics ISFOG 2020. Austin, Texas, USA.

Tasiopoulou, P., K. Ziotopoulou, F. Humire, A. Giannakou, J. Chacko, and T. Travasarou. 2020. "Development and Implementation of Semiempirical Framework for Modeling Postliquefaction Shear Deformation Accumulation in Sands." J Geotech Geoenv Eng, 146 (1). 10.1061/(ASCE)GT.1943-5606.0002179.

Tasiopoulou, P., Y. Chaloulos, N. Gerolymos, A. Giannakou, and J. Chacko. 2021. "Cyclic lateral response of OWT bucket foundations in sand: 3D coupled effective stress analysis with Ta-Ger model." Soils and Foundations, 61 (2): 371–385. https://doi.org/10.1016/J.SANDF.2020.12.002.

Tasiopoulou, P., Y. K. Chaloulos, A. Giannakou, and J. Chacko. 2023. "Seismic performance of sheet-pile wall supporting liquefiable backfill: Blind predictions of centrifuge model tests using Ta-Ger constitutive model." SDEE, 174. Elsevier. https://doi.org/10.1016/J.SOILDYN.2023.108174.

Youd, T. L., I. M. Idriss, R. D. Andrus, I. Arango, G. Castro, J. T. Christian, R. Dobry, W. D. L. Finn, Jr. Leslie F. Harder, M. E. Hynes, K. Ishihara, J. P. Koester, S. S. C. Liao, I. William F. Marcuson, G. R. Martin, J. K. Mitchell, Y. Moriwaki, M. S. Power, P. K. Robertson, R. B. Seed, and I. Kenneth H. Stokoe. 2001. "Liquefaction Resistance of Soils: Summary Report from the 1996 NCEER and 1998 NCEER/NSF Workshops on Evaluation of Liquefaction Resistance of Soils." J Geotech Geoenv Eng, 127 (10)